

## Article

# Reactive, Sparingly Soluble Calcined Magnesia, Tailor-Made as the Reactive Material for Heavy Metal Removal from Contaminated Groundwater Using Permeable Reactive Barrier

Alena Fedoročková \* , Pavel Raschman, Gabriel Sučík, Mária Švandová and Agnesa Doráková

Faculty of Materials, Metallurgy and Recycling, Technical University of Košice, Letná 9, 040 01 Košice, Slovakia; pavel.raschman@tuke.sk (P.R.); gabriel.sucik@tuke.sk (G.S.); ferencovamaria@gmail.com (M.Š.); agnesdorakova@gmail.com (A.D.)

\* Correspondence: alena.fedorockova@tuke.sk; Tel.: +421-55-602-3109

**Abstract:** A laboratory method was designed and verified that allows for the testing of alkaline, magnesite-based reactive materials for permeable reactive barriers (PRBs) to remove heavy metals from contaminated groundwater. It was found that caustic calcined magnesia (CCM) with high reactivity and low solubility to remove  $\text{Cu}^{2+}$ ,  $\text{Zn}^{2+}$ ,  $\text{Ni}^{2+}$ , and  $\text{Mn}^{2+}$  cations from mixed aqueous solutions can be prepared by calcination at a suitable temperature and residence time. Regarding the solubility of both the reactive material itself and the precipitates formed, the CCM should contain just a limited content of lime. One way is the calcination of a ferroan magnesite at temperatures above 1000 °C. However, the decrease in pH is accompanied by lower efficiency, attributed to the solid-phase reactions of free lime. A different way is the calcination of magnesite under the conditions when  $\text{CaCO}_3$  is not thermally decomposed. The virtually complete removal of the heavy metals from the model solution was achieved using the CCM characterised by the fraction of carbonates decomposed of approximately 80% and with the highest specific surface area. CCM calcined at higher temperatures could also be used, but this would be associated with higher consumption of crude magnesite. Under the conditions considered in the present work, the product obtained by the calcination at 750 °C for 3 h appeared to be optimal. The full heavy metal removal was observed in this case using less magnesite, and, moreover, at a lower temperature (resulting, therefore, in a lower consumption of energy for the calcination and material handling).



**Citation:** Fedoročková, A.; Raschman, P.; Sučík, G.; Švandová, M.; Doráková, A. Reactive, Sparingly Soluble Calcined Magnesia, Tailor-Made as the Reactive Material for Heavy Metal Removal from Contaminated Groundwater Using Permeable Reactive Barrier. *Minerals* **2021**, *11*, 1153. <https://doi.org/10.3390/min11111153>

Academic Editors:  
Ana Romero-Freire and Hao Qiu

Received: 7 October 2021  
Accepted: 14 October 2021  
Published: 20 October 2021

**Publisher's Note:** MDPI stays neutral with regard to jurisdictional claims in published maps and institutional affiliations.



**Copyright:** © 2021 by the authors. Licensee MDPI, Basel, Switzerland. This article is an open access article distributed under the terms and conditions of the Creative Commons Attribution (CC BY) license (<https://creativecommons.org/licenses/by/4.0/>).

**Keywords:** groundwater; heavy metal; precipitation; caustic calcined magnesia (CCM); permeable reactive barrier (PRB)

## 1. Introduction

Groundwater is the main source of drinking water worldwide [1,2]. However, there are numerous sites all over the world characterised by groundwater contaminated with organic and/or inorganic compounds, including toxic metals. Groundwater contamination with heavy metals as a consequence of mining, refining, and industrial operations, such as galvanic processing [3], scrubbing of the flue gases in power plants [4], leather tanning [5], improper waste disposal, or accidents in the production of chemicals, represents an important challenge for the authorities responsible for the environmental protection [6,7].

Although some heavy metals, such as copper (Cu), manganese (Mn), and zinc (Zn), are essential for living organisms at specific concentrations, significant amounts can result in shortness of breath, central nervous system disorders, reproductive failure, gastrointestinal problems, and several types of cancers [8–12]. The assimilation of high concentrations of Mn is reported to cause brain malfunction and lead to neurotic disorders [13]. The presence and accumulation of nickel has a toxic or carcinogenic effect on living organisms [14]. Significant amounts of Zn can affect infertility, kidney, and CNS disorders, while overdoses of Cu cause depression and lung cancer [15,16].

In order to reduce the contents of heavy metals in contaminated groundwater, extensive research has been carried out during the last decades to develop efficient and low-cost remediation methods. The conventional solution to this problem considers treatment plants where groundwater is pumped to the land surface and treated using the controlled addition of chemicals, and then redispersed [17]. These “active” techniques, referred to as “pump-and-treat”, require an equipment, maintenance, and supply of energy, carry the risk of exposure to contamination, are unable to remove contaminants adsorbed to the soil [1], and may be impracticable at abandoned sites [18]. An alternative method that is being used increasingly—especially in those areas where the heavy metals are slowly leached from a source [19]—is a permeable reactive barrier (PRB) [4]. In principle, a PRB is a depth filter employing an appropriate granular sparingly soluble reactive material capable of removing the pollutants from the contaminated groundwater as the stream of groundwater passes the PRB [17]. This “passive” treatment system is able to improve water quality by means of precipitation, sorption, or microbial degradation [2,20] using mostly gravitational gradients, practically without any requirements for energy [18].

The most widespread method used to treat acidic metalliferous groundwater is neutralisation (or pH control) [6]. It is well known that the solubility of many cations of metals is reduced in a range of neutral to slightly basic pH, while the solubility can increase in either very acidic or very basic solutions [6,21,22]. Since the minimum solubility of various metals generally occurs at different pH values, the optimum pH for a given contaminated groundwater treatment, which depends on its chemical composition [6], requires a careful control [5,6,23–25]. The minimal solubility of the hydroxides of the majority of metals is reached at a pH between 9.5 and 10.0 [7]. To neutralise an acidic contaminated groundwater, raise its pH, and reach the threshold, the water is brought into contact with an appropriate sparingly soluble alkaline material. It is necessary to guarantee that the optimal pH will be maintained in the barrier during the whole period of its performance [23].

Removing metals via hydroxide precipitation has several advantages: (i) the technology is well-established, simple, and relatively inexpensive; (ii) the ability to achieve the regulatory effluent limits for several metals has been proven; and (iii) non-metal pollutants, such as soaps and fluorides, can be removed [24]. The formation of hydroxides is mostly accompanied by coprecipitation and/or adsorption and gives a mixed precipitate [7,26].

Due to their availability and low cost, limestone [27,28] and lime [2,3,6,24,27] are, in general, the most commonly employed alkaline reactive materials. However, there are certain limitations associated with their use in the PRBs. If, for example, the precipitation of certain metals requires a pH of 8 to 10, limestone is not effective as it only raises the pH to around 8 [6,29]. Moreover, carbon dioxide formed during the limestone dissolution buffers the reactions and makes it difficult to raise the pH even above 6 or 7 [18,30]; although this pH allows for the precipitation of the hydroxides of trivalent metals ( $\text{Fe}^{3+}$ ,  $\text{Al}^{3+}$ ,  $\text{Cr}^{3+}$ ), it is not high enough for divalent metal hydroxides to be formed ( $\text{Fe}^{2+}$ ,  $\text{Zn}^{2+}$ ,  $\text{Mn}^{2+}$ ,  $\text{Cu}^{2+}$ ,  $\text{Pb}^{2+}$ ,  $\text{Ni}^{2+}$ ,  $\text{Co}^{2+}$ , and  $\text{Cd}^{2+}$ ) [18,31–34]. In contrast, both lime and portlandite are unsuitable for passive treatment [31]. They have high solubility as compared to limestone and can raise the pH up to 12–12.5 [2,31,32], which makes some precipitates more soluble [5,24]. Moreover, the use of these substrates results in excessive sludge production and poor settling [27], and the treated, highly alkaline water might thus be harmful to the environment.

An alternative to lime or portlandite is magnesium oxide ( $\text{MgO}$ ), especially in the form of the caustic calcined magnesia (CCM),  $\text{MgO}$ -rich material obtained by the calcination of natural magnesite ( $\text{MgCO}_3$ ) [33]. In relation to the PRBs, CCM is reported to have the following advantages as compared to lime:

- $\text{Mg}(\text{OH})_2$  is much less soluble than  $\text{Ca}(\text{OH})_2$  in aqueous solutions ( $K_{S,\text{Mg}(\text{OH})_2} = 1 \times 10^{-11}$ ;  $K_{S,\text{Ca}(\text{OH})_2} = 4 \times 10^{-6}$ ); it is, therefore, an attractive alternative reagent for passive remediation systems [18].
- Upon contact with water,  $\text{MgO}$  hydrates to form  $\text{Mg}(\text{OH})_2$ , which buffers aqueous solutions' pH between 8.0–10.5 [18,32,33,35]. In this pH range, the solubility of most

metal hydroxides is very low, so divalent metals cations, such as  $Zn^{2+}$ ,  $Cd^{2+}$ ,  $Ni^{2+}$ , or  $Co^{2+}$ , can be removed by precipitation [18,33,35,36].

- MgO has been used for the immobilization of not only the cations of heavy metals but also anionic species, such as borate [26] and fluoride [37], and a strong chemical affinity to arsenic has also been observed [38].
- The residual sludge volume is much lower, mainly due to the elimination of the gypsum formation from sulphate-rich effluents [7,36]; it is easier to be dewatered [24,36] and is less hazardous and, therefore, cheaper to handle [31,32].

The removal of heavy metals from (acidic) aqueous effluents by MgO has been intensively studied by previous authors using synthetic, high-purity (99%) MgO [5,26,37,38], bulk CCM (coarse or fine-grained) [31,32,39,40], or a mixture of a fine-grained CCM and coarse inert matrix (e.g., wood shavings or gravel), so-called dispersed alkaline substrate (DAS) [18,31,33,35,41,42]. The substrates were examined using both laboratory (batch or column) tests [5,18,26,31–33,37–41] and field experiments [35,41,42].

The aim of the present work was to design a laboratory method that allows for:

- (a) testing the reactivity of natural magnesite-based reactive materials for the PRBs;
- (b) defining the conditions for magnesite calcination when the reactive material (CCM) with the optimal reactivity for the removal of the selected heavy metals ( $Cu^{2+}$ ,  $Zn^{2+}$ ,  $Ni^{2+}$ , and  $Mn^{2+}$ ) from contaminated water is obtained.

Though the calcination temperature of pure synthetic  $MgCO_3$  has been found to affect the extent of the MgO hydration [26,37] as well as the immobilization mechanism of borate [26] and fluoride [37], no publications have been published that comprehensively report on how to prepare the MgO from magnesite with the optimal reactivity for the removal of the monitored pollutants.

## 2. Materials and Methods

### 2.1. Materials

Bulk breunneritic magnesite concentrate with particle sizes up to 2 mm, supplied by the company SMZ (Jelšava, Slovakia), was used in the present study. For the laboratory tests, raw magnesite with grain size ranging from 80 to 250  $\mu m$  was obtained by grinding and dry-screening. The content of the main elements in the input (uncalcined) magnesite sample was determined in an external certified chemical laboratory EKOLAB (<https://www.ekolab.sk/certificates> (accessed on 22 May 2003)) using atomic absorption spectrometry (AAS, contrAA<sup>®</sup> 700 Analytik Jena, Jena, Germany). The results of chemical analysis are shown in Table 1.

**Table 1.** Chemical composition of the raw (uncalcined) magnesite.

Element	Mg	Fe	Ca	Si	Al	Loss on Ignition (L.O.I.)
Weight %	25.1	3.0	2.3	0.14	0.10	50.2

### 2.2. Calcination of Magnesite

First, to find the calcination temperature, thermal decomposition of uncalcined raw magnesite was studied by simultaneous differential thermal analysis and thermogravimetric analysis in air atmosphere (DTA/TGA, NETZSCH STA 449 F3 Jupiter, NETZSCH-Gerätebau GmbH, Selb, Germany), and by high-temperature X-ray powder diffraction analysis in high-temperature chamber using  $CoK_{\alpha}$  radiation (X'Pert PRO XL XRD System from PANalytical, Malvern, UK) as well.

Then, the samples of caustic calcined magnesia (CCM) for the batch reactivity tests were prepared as follows: uncalcined raw magnesite was placed in a quartz crucible with a lid and inserted in a laboratory electric high-temperature chamber oven (NETZSCH Model 417, NETZSCH-Gerätebau GmbH, Selb, Germany) where the sample was heated at a pre-defined temperature (between 550 °C and 1400 °C) for a selected time (10–240 min) under static air atmosphere and then cooled down naturally to room temperature in closed oven.

After calcination, the weight of each sample was measured to calculate the weight loss. The calcined products were stored in a vacuum desiccator prior to their use in experiments.

The samples of uncalcined and calcined magnesite were characterised by X-ray powder diffraction by Bragg-Bretano  $\Theta$ – $2\Theta$  geometry (XRD, Rigaku, MiniFlex 600 diffractometer, Akishima, Japan) using  $\text{CuK}\alpha$  radiation at 40 kV and 15 mA at a step of  $0.01^\circ$  and speed of  $2^\circ \text{ min}^{-1}$  specified by PDXL2, ver. 2.6.1.2 software with the Powder Diffraction File (PDF-2, ver. 2.1502, Newtown Square, PA, USA) databases from International Centre for Diffraction Data (ICDD). Measurements of the specific surface area were performed using the  $\text{N}_2$ -adsorption B.E.T. method (NOVA 1000 Quantachrome Instrument, Boynton Beach, FL, USA).

### 2.3. Batch Precipitation Tests

The reactivity of prepared CCM was tested using its reaction with a model mixed aqueous solution of  $\text{Cu}^{2+}$ ,  $\text{Zn}^{2+}$ ,  $\text{Ni}^{2+}$ , and  $\text{Mn}^{2+}$  at  $25^\circ\text{C}$ . The initial concentration of each cation in the used model mixed solution was approx. 50 mg/L, and the initial pH was 5.1. The model mixed solution was prepared by dissolving the sulphates of  $\text{Cu}^{2+}$ ,  $\text{Zn}^{2+}$ ,  $\text{Ni}^{2+}$ , and  $\text{Mn}^{2+}$  (special grade, Sigma-Aldrich, St. Louis, MO, USA) in distilled water. In each test, a defined amount (0.2 g) of prepared CCM was added to 40 mL of the model solution (liquid:solid ratio = 200:1) in a plastic bottle and horizontally shaken on a rotary shaker at  $50 \text{ min}^{-1}$  and  $25^\circ\text{C}$  for 2 h. (In preliminary experiments, it was observed that the equilibrium was achieved within 10 to 90 min under the conditions used). Then, the slurry was filtered (Munktell Filtrak (Quant.) Grade: 389;  $84 \text{ g/m}^2$ ; 8–12  $\mu\text{m}$  pore size), and the final pH was measured in the filtrate by a pH meter (HI4222, Hanna Instruments, Nusfalau, Romania) by ORP electrode (HI3131B, Hanna Instruments, Nusfalau, Romania). The initial concentrations of metal ions in the model mixed solution and the residual concentrations of dissolved metal ions in the filtrate were verified and determined by inductively coupled plasma-atomic emission spectrometry (ICP-OES, Thermo Scientific iCAP 6000 DUO, Thermofisher Scientific, Cambridge, UK). The single element solution standards (1000 ppm in  $\text{HNO}_3$ , Fisher Scientific UK, Leics, UK) for calibration were used. The efficiency of individual metals removal ( $E_i$ ) was calculated using Equation (1):

$$E_i = \frac{c_{i,0} - c_{i,r}}{c_{i,0}} \quad (1)$$

where  $c_{i,0}$  is the initial concentration (mg/L) and  $c_{i,r}$  is the final concentration (mg/L) of each cation  $i = \text{Cu}^{2+}$ ,  $\text{Ni}^{2+}$ ,  $\text{Mn}^{2+}$ , and  $\text{Zn}^{2+}$  in the model mixed solution. The results are presented as the average of three repeated measurements.

## 3. Results and Discussion

The major mineral phases identified in the raw magnesite sample by the X-ray powder diffraction method (Figure 1) were: magnesite (00-008-0479 PDF-2 card), ferroan variety of magnesite (00-036-0383 PDF-2 card) representing the solid solution of magnesite ( $\text{MgCO}_3$ ) and siderite ( $\text{FeCO}_3$ ) and characterised by the formula  $(\text{Mg,Fe})\text{CO}_3$ , where the Mg:Fe atomic ratio ranged from 90:10 to 70:30, and dolomite (00-036-0426 PDF-2 card). The minor phases were calcite (00-004-0636 PDF-2 card) and enstatite (00-002-0520 PDF-2 card).

### 3.1. Thermal Decomposition of Magnesite

The results of the thermal analysis (Figure 2) showed that the thermal decomposition of the magnesite started at  $440^\circ\text{C}$ , and the maximum endothermic effect (corresponding to the maximum rate of the thermal decomposition of the magnesite mineral) was observed at  $660^\circ\text{C}$ . The second endothermic effect contains two hidden peaks with an onset at  $697^\circ\text{C}$ , indicated by the subsequent thermal decomposition of the dolomitic part of the crude magnesite. The total observed weight loss due to the release of the carbon dioxide was 50.2 wt.%.

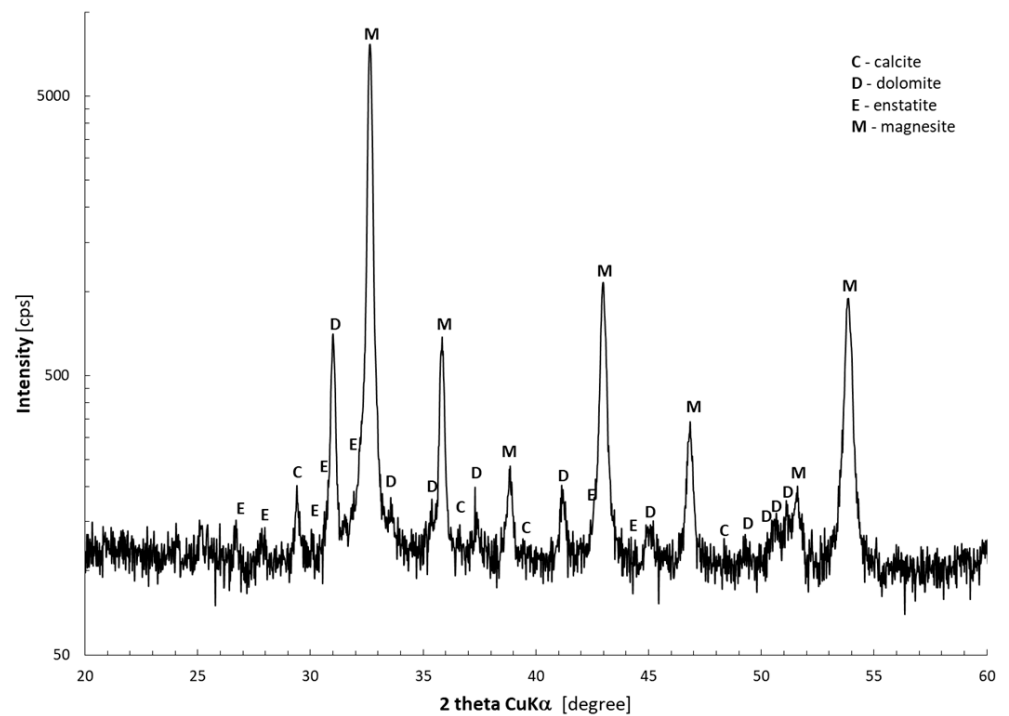


**Figure 1.** XRD analysis of the raw magnesite used for the experiments.

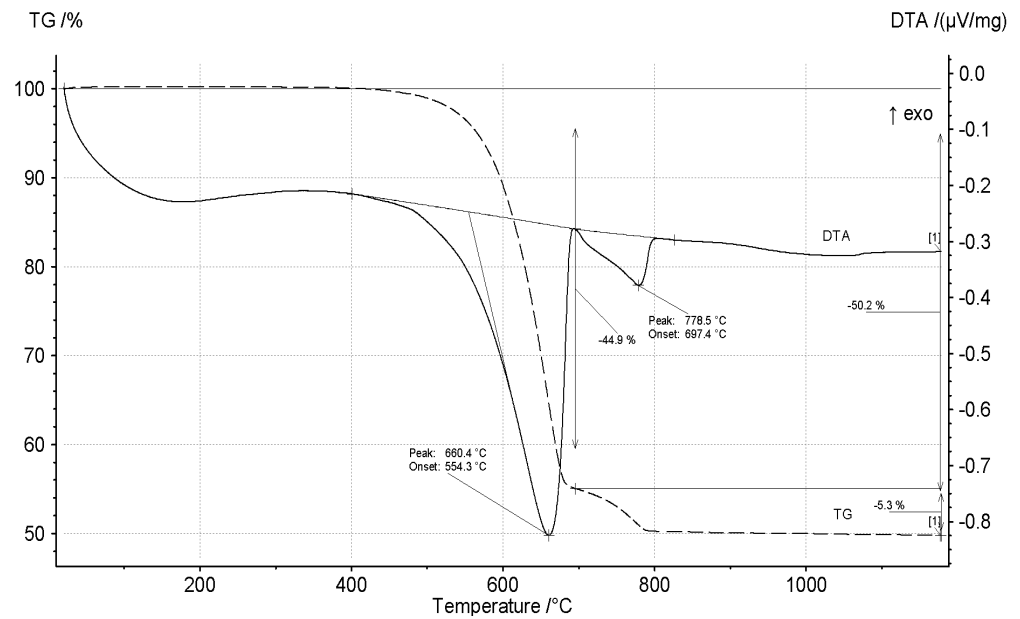


**Figure 2.** Results of thermal analysis illustrating the thermal decomposition of magnesite and dolomite during heating the raw magnesite.

The influence of the calcination temperature between 400 and 1200 °C on the phase composition and crystallinity is illustrated in Figure 3. Between 600 and 800 °C, the phases of magnesite and dolomite originally present gradually disappeared, and the structure of the calcined sample appeared to be highly disordered. Starting from 600 °C, the XRD count from the magnesite got progressively lower and practically disappeared at 800 °C. The dolomitic part of the raw magnesite decomposed at temperatures above 700 °C, and no dolomite could actually be identified at 800 °C. At temperatures above 700 °C, new phases (mainly periclase, MgO) occurred.

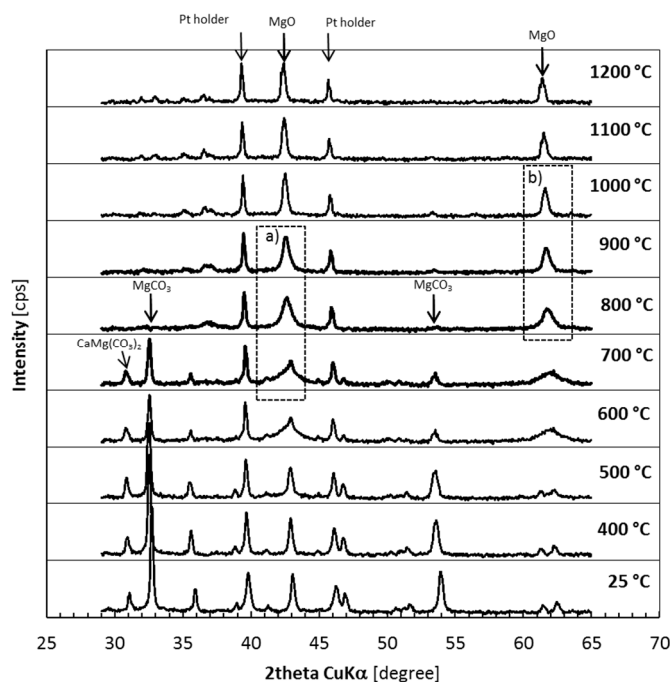


**Figure 3.** In situ high-temperature X-ray powder diffraction sequence illustrating the changes in phase composition and crystallinity during heating the raw magnesite. (Magnesite and dolomite reflections gradually disappear above 700 °C (frame “a”), and the new phase of periclase is created (frame “b”).).

The DTA, TGA, and XRD analyses suggest that the samples should be calcined at temperatures between 600 and 900 °C to produce a reactive form of magnesia.

The effect of the calcination temperature (from 550 °C to 1000 °C) and time (from 10 min to 4 h) on the thermal decomposition of the carbonates present in the crude (uncalcined) magnesite are illustrated in Figure 4.

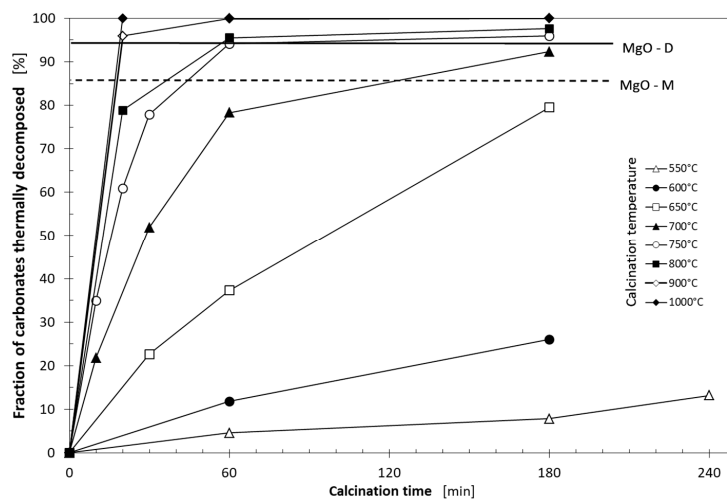


**Figure 4.** Influence of temperature and time on fraction of carbonates decomposed during heating the raw magnesite.

The fraction of the carbonates thermally decomposed,  $X_t$ , was calculated for each calcined sample using the following relationship (Equation (2)):

$$X_t = \frac{100}{w_0} \cdot \frac{m_0 - m_t}{m_0} \tag{2}$$

where  $m_0$  is the weight of the sample before calcination (equal to 40 g),  $m_t$  is the weight of the sample after calcination, and  $w_0$  is the total content of the carbon dioxide chemically bonded in the form of carbonates in the original (uncalcined) magnesite rock (represented by the L.O.I. and equal to 50.2 wt.%).

Two horizontal lines in Figure 4 represent the two limits, which are as follows: the dashed line (MgO-M) = the thermal decomposition of the magnesite was completed and the decomposition of the  $\text{MgCO}_3$  from the dolomitic part just started; the full line (MgO-D) = the thermal decomposition of the  $\text{MgCO}_3$  from the dolomitic part was completed and the decomposition of the  $\text{CaCO}_3$  just started.

Figure 4 shows that, at a temperature of 550 °C, the fraction of the carbonates thermally decomposed,  $X_t$ , reached 13% after 4 h. At temperatures above 900 °C, the carbonates were almost completely decomposed within 1 h.

### 3.2. Removal of Heavy Metals by Precipitation Using the CCM

The influence of the calcination temperature and time on the efficiency ( $E_i$ ) of the  $\text{Cu}^{2+}$ ,  $\text{Zn}^{2+}$ ,  $\text{Ni}^{2+}$ , and  $\text{Mn}^{2+}$  removal from the model mixed solution by the addition of a sample of the prepared CCM as a precipitating agent is illustrated in Figure 5a–d. The accuracy of the measurements expressed as %RSD ranged from 0.2% to 0.8% depending on the wavelengths of the selected emission lines.

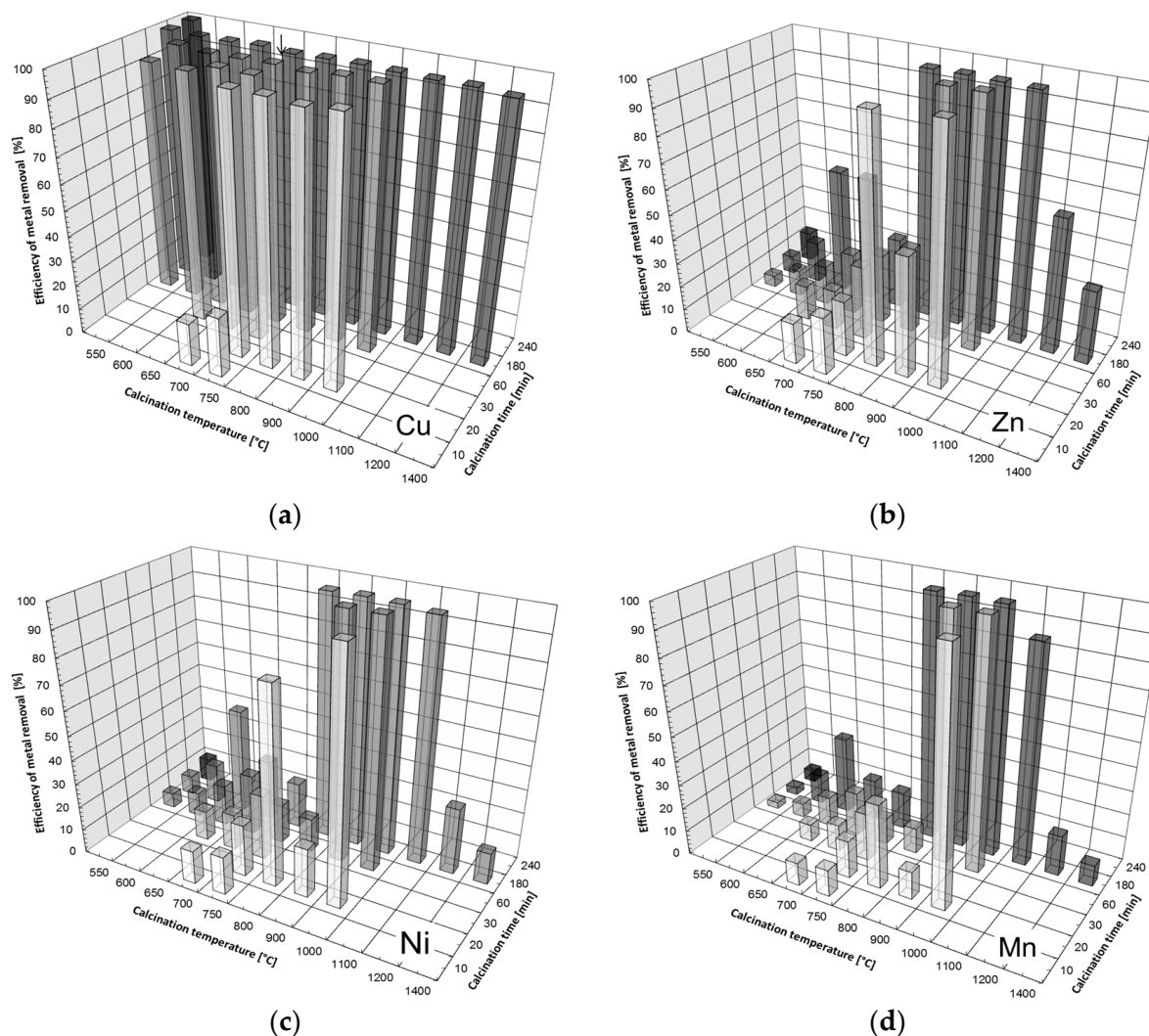


**Figure 5.** Influence of calcination temperature and time on the efficiency of monitored metal removal from the model solution by addition of the CCM tested: (a)  $\text{Cu}^{2+}$ , (b)  $\text{Zn}^{2+}$ , (c)  $\text{Ni}^{2+}$ , and (d)  $\text{Mn}^{2+}$  using a liquid-to-solid ratio  $l:s = 200:1$ .

A comparison of the graphs in Figure 5a–d suggests that the behaviours of Zn, Ni, and Mn were very similar, but quite different from that of Cu. After an addition of the CCM, the copper was completely precipitated (Figure 5a) with the exception of the three cases where the magnesite had not been thermally activated enough due to the low calcination temperature and/or short calcination time (samples 550 °C for 1 h, 700 °C for 10 min, and 750 °C for 10 min). In contrast, the efficiency of the removal of the Zn, Ni, and Mn first grew with the calcination temperature and time and reached approximately 100% at a calcination temperature of 800 °C to 1000 °C and sufficiently long calcination time (from 20 min at 1000 °C up to 3 h at 800 °C), and then decreased at temperatures above 1100 °C (Figure 5b–d).

The comparison of the results in Figure 5 shows that the most reactive material, which would achieve a comprehensive removal of all the monitored metals, can be prepared by calcination at temperatures above 800 °C. These results are in good agreement with the final pH values (measured in the filtrate at the end of each test) that are shown in Figure 6.

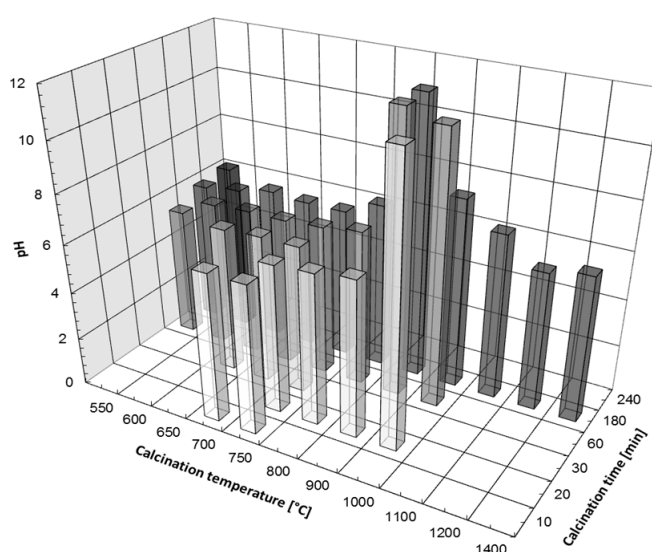
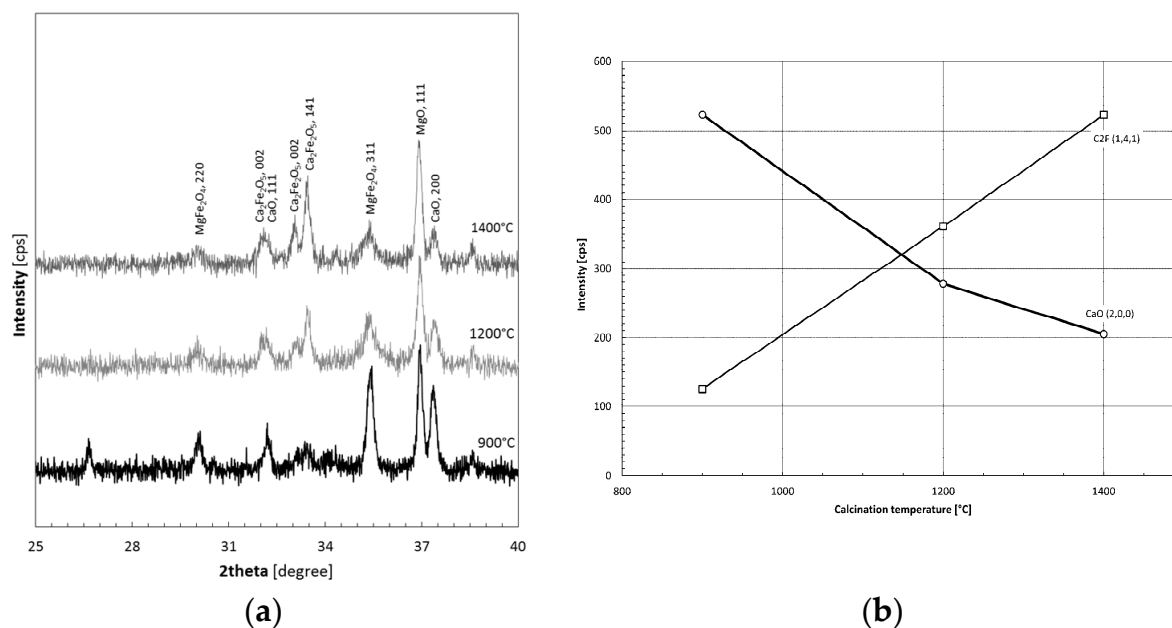


Figure 6. Final pH measured at the end of individual precipitation tests.

The highest final values of the pH in Figure 6 correlate very well with the maximum values of the efficiency of the individual metal removal,  $E_i$ , in Figure 5b–d. However, the highest observed final values of the pH (up to 11.5) cannot be attributed to  $\text{Mg}(\text{OH})_2$ , which buffers aqueous solutions to a pH between 8.0–10.5 [18,32,33,35]. It can, therefore, be assumed that these high pH values are due to the presence of free lime, which is formed in the samples calcined above 800 °C as a product of the thermal decomposition of the dolomite and/or calcite originally present in the raw magnesite used.

To be able to explain the changes in the reactivity of the CCM prepared, a comprehensive analysis of the changes taking place in the raw magnesite during the calcination is needed.

The results of the phase analysis (Figure 7a) showed that, at a temperature of 900 °C, the free lime is formed as a product of the thermal decomposition of the dolomite and/or calcite originally present in the used raw magnesite. In addition, from the diffractograms shown in Figure 7a, it can be seen that the calcination at very high temperatures (above 1000 °C) results in the solid-phase reaction of the free lime ( $\text{CaO}$ ) and the formation of dicalcium ferrite ( $2\text{CaO}\cdot\text{Fe}_2\text{O}_3$ ), as illustrated by the graph in Figure 7b, while the XRD counts from the  $\text{CaO}$  (200) were getting progressively lower with an increase in the calcination temperature; those from the  $2\text{CaO}\cdot\text{Fe}_2\text{O}_3$  (141) were simultaneously increased. The conversion of the  $\text{CaO}$  to  $2\text{CaO}\cdot\text{Fe}_2\text{O}_3$  explains the gradual decrease in the reactivity of the products calcined at temperatures above 1000 °C (Figure 5b–d).



**Figure 7.** Results of phase analysis illustrating the solid-phase chemical reactions occurring during heating the raw magnesite: (a) identified products at various temperatures, (b) conversion of free lime to dicalcium ferrite ( $2\text{CaO}\cdot\text{Fe}_2\text{O}_3$ ).

The CCM intended for use as a reactive material in the PRB should contain just a limited content of CaO in the form of lime. This limit is determined by the demands on a proper performance of the PRB. The presence of the lime in the CCM can become significant, especially when raw magnesite with a higher CaO content is used. Although calcination at temperatures up to 1000 °C leads to a seemingly higher efficiency of heavy metal removal (Figure 5), this effect is at the expense of the benefits resulting from the low solubility of MgO. The presence of the lime results in high pH values (pH up to 12–12.5) that make some precipitates more soluble [5,24]. Moreover, highly alkaline water might be harmful to the environment.

One way to reduce the lime content in the CCM is the calcination of the magnesite at very high temperatures; at temperatures above 1000 °C, a decrease in the pH values was observed (Figure 6), accompanied by lower efficiency (Figure 5), which may be attributed to the solid-phase reaction of the free lime (CaO) and the formation of dicalcium ferrite ( $2\text{CaO}\cdot\text{Fe}_2\text{O}_3$ ) (Figure 7a,b).

A different way to avoid overly high lime content in the CCM is the calcination of the magnesite under the conditions when  $\text{CaCO}_3$  is not thermally decomposed. The graph in Figure 8 shows the removal efficiencies of the individual metals (shown in Figure 5) depending on the amount of crude magnesite that has to be calcined to treat 1 m<sup>3</sup> of contaminated water with the same composition as the model solution used. Maintaining the same conditions (the composition of the liquid and solid phase, 1:s ratio = 200:1) as used in the laboratory tests, 5 kg of calcined magnesite would be necessary to treat 1 m<sup>3</sup> of the model solution used. The mass of crude magnesite to produce 5 kg of the CCM under the given calcination temperature and time was calculated using Equation (3):

$$m_{\text{crude magnesite}} = \frac{500 \text{ kg}}{100 - 0.502X_t} \quad (3)$$

From Figure 8, it can be seen that the efficiency of the removal of the individual metals by the addition of the calcined magnesite decreased in the order  $\text{Cu} \gg \text{Zn} > \text{Ni} > \text{Mn}$ . This finding is in accordance with the fact that a hydroxide with a lower value of the solubility product is preferably precipitated. The values of the solubility products of the hydroxides of the monitored metals decrease in the following order:  $\text{Cu}(\text{OH})_2 < \text{Zn}(\text{OH})_2 < \text{Ni}(\text{OH})_2 < \text{Mn}(\text{OH})_2$ .

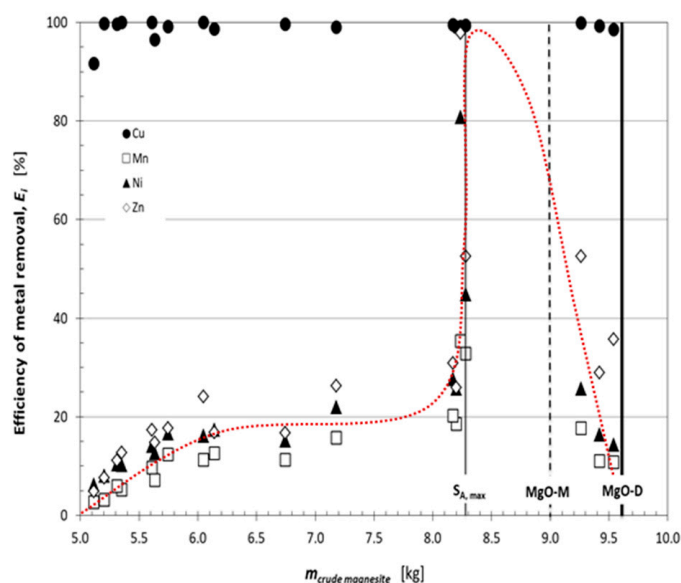


**Figure 8.** Efficiency of individual metals removal,  $E_i$ , in dependence on the amount of crude magnesite,  $m_{\text{crude magnesite}}$ , consumed to prepare the CCM under different calcination temperature and time. (Experimental conditions: Total heavy metal concentration at the beginning of each precipitation test =  $3.33 \text{ mol m}^{-3}$ ; l:s ratio = 200:1. Dotted curve = regression curve).

From the course of the dependences  $E_i = f_i(m_{\text{magnesite}})$  in Figure 8 (and Equation (3): the higher  $X_t$ , the higher  $m_{\text{crude magnesite}}$ ), it follows that  $E_i$  was initially increased with an increase in  $X_t$  of the added calcined magnesite: the practically complete precipitation of the copper occurred already after the addition of the CCM characterised by  $X_t$  of approximately 8%, while the efficiency  $E_i$  of Zn, Ni, and Mn was first growing rapidly with increasing  $X_t$ , then the rise of  $E_i$  was slowed down. At  $m_{\text{crude magnesite}} = 8.3 \text{ kg}$  ( $X_t = 79\%$ ),  $E_i$  reached the maximum (characterised by the step-wise increase in  $E_i$ ). When the conversion  $X_t$  was assigned to the corresponding value of the specific surface area shown in Figure 9, it was found that the maximum efficiency  $E_i$  was achieved by the addition of the CCM with the largest specific surface area. This limit is marked in Figure 8 with a full vertical line ( $S_{A,MAX}$ ). (The specific surface area reached the maximum of  $112 \text{ m}^2 \cdot \text{g}^{-1}$  at the calcination temperature of  $750 \text{ }^\circ\text{C}$  and time 30 min, where  $X_t = 79\%$ ). Then, until the  $\text{MgCO}_3$  in the raw magnesite was completely decomposed (this limit is marked with the dashed vertical line (MgO-M) in both Figures 4 and 8), the efficiency  $E_i$  remained almost constant and close to its maximum value. At last, despite the increasing content of the MgO,  $E_{Zn}$  was very slowly getting higher, while the efficiencies for Ni and Mn were decreasing at the same time. The drop in the efficiency is likely to be caused by: (i) the recrystallisation of the periclase and (ii) the loss of the reactive MgO due to its solid-phase reaction with the  $\text{Fe}_2\text{O}_3$  to produce magnesium ferrite ( $\text{MgO} \cdot \text{Fe}_2\text{O}_3$ ) (Figure 7a).

The above results show that the virtually complete removal of the heavy metals from the model solution can be achieved with the addition of CCM characterised by the fraction of carbonates decomposed  $X_t = 79\%$  and the highest specific surface area. Under the conditions of this work, the magnesite was calcined at  $750 \text{ }^\circ\text{C}$  for 3 h. Magnesite calcined at higher temperatures could also be used, but this would be associated with the higher consumption of the crude magnesite to prepare the same amount of the CCM. Approximately 8.3 kg of crude magnesite calcined at  $750 \text{ }^\circ\text{C}$  for 3 h, but up to 10.0 kg of magnesite calcined at  $1000 \text{ }^\circ\text{C}$  for 20 min would be consumed to prepare 5 kg of CCM to remove the heavy metals from  $1 \text{ m}^3$  of the model solution. The higher specific consumption of crude magnesite brings increased handling and heating costs, and the higher degree of carbonate decomposition ( $X_t$ ) increases the calcination costs (thermal decomposition). The product obtained by calcination at  $750 \text{ }^\circ\text{C}$  for 3 h, therefore, appears to be optimal: it is enough to decompose only 80% of the  $\text{MgCO}_3$  present in the magnesite at a lower

temperature (therefore, less energy is needed for calcination), and the same amount of heavy metals can be precipitated by adding 1 t of this material as by adding 1 t of the CCM obtained at higher temperatures.

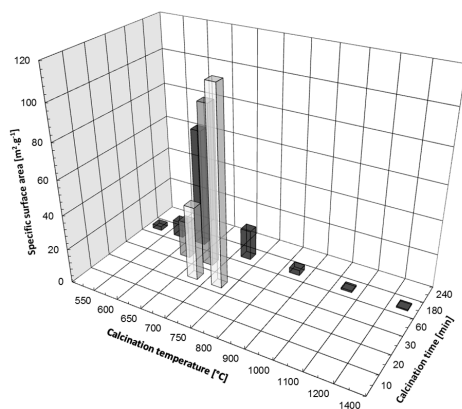
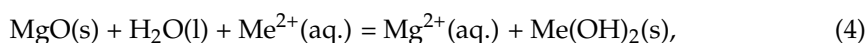
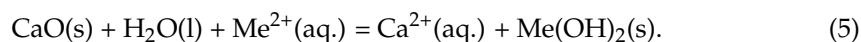


**Figure 9.** Influence of calcination temperature and time on specific surface area during heating the raw magnesite.

It is assumed that the removal of heavy metals from aqueous solutions by the addition of CCM is based on precipitation, according to the overall chemical equation:



eventually,



This assumption is based on the fact that, at the end of each test, the  $\text{Mg}^{2+}$  and  $\text{Ca}^{2+}$  contents in the final solution were also determined. The results showed that the  $\text{Mg}^{2+} + \text{Ca}^{2+}$  contents corresponded within the experimental error to the total amount of heavy metals removed from the solution during the test. This conclusion differs from the findings of Sasaki et al. [26,37], who used the reactive  $\text{MgO}$  obtained by the calcination of pure (synthetic)  $\text{MgCO}_3$  as a reactive material for the removal of fluoride and borate. Sasaki et al. [26,37] found that the efficiency did not depend on a specific surface but the critical factor was the basicity per unit surface area, which was gradually getting higher in the range of the calcination temperature between 600 °C and 1100 °C. The reason(s) for this difference may be:

- (a) the differences in the nature of the starting materials used: natural magnesite was used in this work;
- (b) the differences between the products of calcination: the calcined magnesite prepared and used in this work was characterised by a high internal surface to external surface ratio;
- (c) the different mechanism of the heavy metals removal: while adsorption was identified in the work of Sasaki et al. [17,28], precipitation prevailed in the present work, which was proved by high contents of  $\text{Mg}^{2+} + \text{Ca}^{2+}$  cations in the final solutions when the reaction (phase contact) was stopped.

#### 4. Conclusions

The caustic calcined magnesite (CCM) can be applied as an alkaline reactive material in permeable reactive barriers (PRBs) with dispersed alkaline substrate, designed for the removal of heavy metals from contaminated groundwater. There are two crucial properties that characterise an appropriate CCM for this application: high reactivity and low solubility. The present work reports on how the tailor-made CCM for use in the PRBs can be prepared by the thermal activation of the natural magnesite. It was found out that the CCM with the required reactivity for the removal of the  $\text{Cu}^{2+}$ ,  $\text{Zn}^{2+}$ ,  $\text{Ni}^{2+}$ , and  $\text{Mn}^{2+}$  cations from a

model mixed aqueous solution can be obtained by a suitable adjustment of the calcination temperature and time.

Regarding the solubility, the CCM should contain just a limited content of CaO in the form of lime, which is produced by the thermal decomposition of CaCO<sub>3</sub>. This limit is determined by the demands on a proper performance of the PRB. Although the calcination at temperatures up to 1000 °C practically results in full heavy metal removal, this effect is at the expense of the benefits resulting from the low solubility of MgO. The presence of lime results in high pH values (pH up to 12–12.5) that make some precipitates more soluble. Moreover, highly alkaline purified water might be harmful to the environment.

One way to reduce the lime content in the CCM is the calcination of magnesite at very high temperatures. At the temperatures above 1000 °C, a decrease in the pH values was observed. However, the decrease in pH was accompanied by lower efficiency, attributed to the solid-phase reaction of free lime (CaO) to form the dicalcium ferrite (2CaO·Fe<sub>2</sub>O<sub>3</sub>).

A different way to avoid high lime content in the CCM is the calcination of magnesite under the conditions when CaCO<sub>3</sub> is not thermally decomposed. The results have shown that the virtually complete removal of the heavy metals from the model solution was achieved using the CCM characterised by the fraction of the carbonates decomposed  $X_t = 79\%$  and the highest specific surface area. Under the conditions of this work, the magnesite was calcined at 750 °C for 3 h. Magnesite calcined at higher temperatures could also be used, but this would be associated with a higher consumption of crude magnesite to prepare the same amount of the CCM. The higher specific consumption of crude magnesite brings increased handling and heating costs, and the higher degree of carbonate decomposition increases the calcination costs (thermal decomposition).

Whether to choose the operation conditions for the calcination when the calcium carbonate is also decomposed or not depends on the composition of the magnesite used and the overall cost of the CCM production. However, to verify the designed laboratory method for testing the reactivity of the CCM-based reactive materials for the PRBs, the product obtained by calcination at 750 °C for 3 h appeared to be optimal. Adding 1 t of this material allowed for the same amount of heavy metals precipitated as adding 1 t of the CCM obtained at higher temperatures. At the same time, it was enough to decompose only 80% of the MgCO<sub>3</sub> present in the magnesite at a lower temperature (resulting in a lower consumption of energy for the calcination and material handling).

**Author Contributions:** Conceptualization, P.R., G.S. and A.F.; methodology, P.R.; software, G.S.; validation, A.F., A.D. and M.Š.; formal analysis, A.D.; investigation, A.D., M.Š.; resources, A.F.; data curation, P.R.; writing—original draft preparation, A.F., P.R.; writing—review and editing, P.R., A.F.; visualization, G.S.; supervision, P.R.; project administration, A.F.; funding acquisition, P.R. All authors have read and agreed to the published version of the manuscript.

**Funding:** This work was financially supported by the Scientific Grant Agency of the Ministry of Education of the Slovak Republic and the Slovak Academy of Sciences (VEGA 1/0176/19).

**Acknowledgments:** The authors thank Beatrice Plešingerová for specific surface analysis.

**Conflicts of Interest:** There are no conflict to declare.

## Abbreviations

CCM	caustic calcined magnesia
PRB	permeable reactive barrier
HM	heavy metals
DAS	dispersed alkaline substrate, i.e., mixture of a fine-grained caustic calcined magnesia and coarse inert matrix (e.g., wood shavings or gravel)
$E_i$	efficiency of individual heavy metals removal from solution (%)
$X_t$	fraction of carbonates thermally decomposed during the raw magnesite heating (%)

## References

1. Permeable Reactive Barriers for Inorganic and Radionuclide Contamination. Kate Bronstein National Network of Environmental Management Studies Fellow for U.S. Environmental Protection Agency Office of Solid Waste and Emergency Response Office of Superfund Remediation and Technology Innovation, Washington, DC, August 2005. Available online: <https://clu-in.org/download/studentpapers/bronsteinprbpaper.pdf/> (accessed on 30 November 2016).
2. Thiruvenkatachari, R.; Vigneswaran, S.; Naidu, R. Permeable reactive barrier for groundwater remediation. *J. Ind. Eng. Chem.* **2008**, *14*, 145–156. [[CrossRef](#)]
3. Fu, F.; Wang, Q. Removal of heavy metal ions from wastewaters: A review. *J. Environ. Manag.* **2011**, *92*, 407–418. [[CrossRef](#)]
4. Johnson, D.B.; Hallberg, K.B. Acid mine drainage remediation options: A review. *Sci. Total Environ.* **2005**, *338*, 3–14. [[CrossRef](#)]
5. Barbooti, M.M.; Abid, B.A.; Al-Shuwaiki, N.M. Removal of heavy metals using chemicals precipitation. *Eng. Tech. J.* **2011**, *29*, 595–612.
6. Taylor, J.; Pape, S.; Murphy, N. A Summary of Passive and Active Treatment Technologies for Acid and Metalliferous Drainage (AMD), Fifth Australian Workshop on Acid Drainage, 29–31 August 2005 Fremantle, Western Australia. The Australian Centre for Minerals Extension and Research (ACMER), Earth Systems PTY Ltd., Australian Business Number 29 006 227 532. Available online: [http://www.earthsystems.com.au/wp-content/uploads/2012/02/AMD\\_Treatment\\_Technologies\\_06.pdf/](http://www.earthsystems.com.au/wp-content/uploads/2012/02/AMD_Treatment_Technologies_06.pdf/) (accessed on 30 November 2016).
7. Blais, J.F.; Djedidi, Z.; Ben Cheikh, R.; Tyagi, R.D.; Mercier, G. Metals precipitation from effluents: Review. *Pract. Period. Hazard. Toxic Radioact. Waste Manag.* **2008**, *12*, 135–149. [[CrossRef](#)]
8. Cantor, K.P. Drinking water and cancer. *Cancer Causes Control.* **1997**, *8*, 292–308. [[CrossRef](#)] [[PubMed](#)]
9. Calderon, R.L. The epidemiology of chemical contaminants of drinking water. *Food Chem. Toxicol.* **2000**, *38*, 13–20. [[CrossRef](#)]
10. Kavcar, P.; Sofuoglu, A.; Sofuoglu, S.C. A health risk assessment for exposure to trace metals via drinking water ingestion pathway. *Int. J. Hyg. Environ. Health* **2009**, *212*, 216–227. [[CrossRef](#)]
11. Kelly, B.C.; Myo, A.N.; Pi, N.; Bayen, S.; Leakhena, P.C.; Chou, M.; Tan, B.H. Human exposure to trace elements in central Cambodia: Influence of seasonal hydrology and food-chain bioaccumulation behaviour. *Ecotox. Environ. Saf.* **2018**, *162*, 112–120. [[CrossRef](#)] [[PubMed](#)]
12. Wu, G.; Kang, H.; Zhang, X.; Shao, H.; Chu, L.; Ruan, C. A critical review on the bio-removal of hazardous heavy metals from contaminated soils: Issues, progress, eco-environmental concerns and opportunities. *J. Hazard. Mater.* **2010**, *174*, 1–8. [[CrossRef](#)] [[PubMed](#)]
13. Nthunya, L.N.; Masheane, M.L.; George, M.; Kime, M.B.; Mhlanga, S.D. Removal of Fe and Mn from polluted water sources in Lesotho using modified clays. *J. Water Chem. Technol.* **2019**, *41*, 81–86. [[CrossRef](#)]
14. Yang, S.; Li, J.; Shao, D.; Hu, J.; Wang, X. Adsorption of Ni (II) on oxidized multi-walled carbon nanotubes: Effect of contact time, pH, foreign ions and PAA. *J. Hazard. Mater.* **2009**, *166*, 109–116. [[CrossRef](#)] [[PubMed](#)]
15. Rehman, I.; Ishaq, M.; Ali, L.; Khan, S.; Ahmad, I.; Ud Din, I.; Ullah, H. Enrichment, spatial distribution of potential ecological and human health risk assessment via toxic metals in soil and surface water ingestion in the vicinity of Sewakht mines, district Chitral, Northern Pakistan. *Ecotox. Environ. Saf.* **2018**, *154*, 127–136. [[CrossRef](#)]
16. Sani, H.A.; Ahmad, M.B.; Hussein, M.Z.; Ibrahim, N.A.; Musa, A.; Saleh, T.A. Nanocomposite of ZnO with montmorillonite for removal of lead and copper ions from aqueous solutions. *Process Saf. Environ. Protect.* **2017**, *109*, 97–105. [[CrossRef](#)]
17. Gibert, O.; De Pablo, J.; Cortina, J.L.; Ayora, C. In situ removal of arsenic from groundwater by using permeable reactive barriers of organic matter/limestone/zero-valent iron mixtures. *Environ. Geochem. Health* **2010**, *32*, 373–378. [[CrossRef](#)] [[PubMed](#)]
18. Rötting, T.S.; Ayora, C.; Carrera, J. Improved passive treatment of high Zn and Mn concentrations using caustic magnesia (MgO): Particle size effects. *Environ. Sci. Technol.* **2008**, *42*, 9370–9377. [[CrossRef](#)] [[PubMed](#)]
19. Simon, F.; Meggyes, T. Removal of organic and inorganic pollutants from groundwater using permeable reactive barriers. *Land Contam. Reclam.* **2000**, *8*, 103–116.
20. Hashim, M.A.; Mukhopadhyay, S.; Sahu, J.N.; Sengupta, B. Remediation technologies for heavy metal contaminated ground water. *J. Environ. Manag.* **2011**, *92*, 2355–2388. [[CrossRef](#)] [[PubMed](#)]
21. Permeable Reactive Barriers: Lessons Learned/New Directions. Interstate Technology & Regulatory Council: Washington, DC, USA, 2005; p. 9. Available online: <http://www.itrcweb.org/GuidanceDocuments/PRB-4.pdf/> (accessed on 30 November 2016).
22. Lee, M.K.; Saunders, J.A. Effects of pH on metals precipitation and sorption: Field bioremediation and geochemical modeling approaches. *Vadose Zone J.* **2003**, *2*, 177–185.
23. Obiri-Nyarko, F.; Grajales-Mesa, S.J.; Malina, G. An overview of permeable reactive barriers for in situ sustainable groundwater remediation. *Chemosphere* **2014**, *111*, 243–259. [[CrossRef](#)]
24. Army Corps. Engineering Manuals, Manual No. 1110-1-4012: Engineering and Design Precipitation/Coagulation/Flocculation, Department of the Army U.S. Army Corps of Engineers, 2001, Washington, DC 20314-1000. Available online: [http://www.publications.usace.army.mil/Portals/76/Publications/EngineerManuals/EM\\_1110-1-4012.pdf/](http://www.publications.usace.army.mil/Portals/76/Publications/EngineerManuals/EM_1110-1-4012.pdf/) (accessed on 30 November 2016).
25. Peters, R.W.; Shem, L. Separation of Heavy Metals: Removal from Industrial Wastewaters and Contaminated Soil. In Proceedings of the Symposium on Emerging Separation Technologies for Metals and Fuels, Palm Coast, FL, USA, 13–18 March 1993. Available online: <http://www.osti.gov/scitech/servlets/purl/6504209-mKij3S/> (accessed on 30 November 2016).
26. Sasaki, K.; Moriyama, S. Effect of calcination temperature for magnesite on interaction of MgO-rich phases with boric acid. *Ceram. Int.* **2014**, *40*, 1651–1660.

27. Barakat, M.A. New trends in removing heavy metals from industrial wastewater. *Arab. J. Chem.* **2011**, *4*, 361–377. [[CrossRef](#)]
28. Skousen, J. Anoxic limestone drains for acid mine drainage treatment. *Green Lands* **1991**, *21*, 30–35.
29. Golab, A.N.; Peterson, M.A.; Indraratna, B. Selection of potential reactive materials for a permeable reactive barrier for remediating acidic groundwater in acid sulphate soil terrains. *Q. J. Eng. Geol. Hydrogeol.* **2006**, *39*, 209–223. [[CrossRef](#)]
30. Akcil, A.; Koldas, S. Acid mine drainage (AMD): Causes, treatment and case studies. *J. Clean. Prod.* **2006**, *14*, 1139–1145. [[CrossRef](#)]
31. Cortina, J.L.; Lagreca, I.; De Pablo, J. Passive in situ remediation of metal-polluted water with caustic magnesia: Evidence from column experiments. *Environ. Sci. Technol.* **2003**, *37*, 1971–1977. [[CrossRef](#)] [[PubMed](#)]
32. Rötting, T.; Cama, J.; Ayora, C.; Cortina, J.L.; De Pablo, J. The Use of Caustic Magnesia to Remove Cadmium from Water. In Proceedings of the 9th International Mine Water Association Congress, Oviedo, Spain, 5–7 September 2005; pp. 635–639. Available online: [http://www.imwa.info/docs/imwa\\_2005/IMWA2005\\_090\\_Roetting.pdf/](http://www.imwa.info/docs/imwa_2005/IMWA2005_090_Roetting.pdf/) (accessed on 30 November 2016).
33. Caraballo, M.A.; Rötting, T.S.; Silva, V. Implementation of an MgO-based metal removal step in the passive treatment system of Shilbottle, UK: Column experiments. *J. Hazard. Mater.* **2010**, *181*, 923–930. [[CrossRef](#)]
34. Macías, F.; Caraballo, M.A.; Nieto, J.M.; Rötting, T.S.; Ayora, C. Natural pretreatment and passive remediation of highly polluted acid mine drainage. *J. Environ. Manag.* **2012**, *104*, 93–100. [[CrossRef](#)] [[PubMed](#)]
35. Caraballo, M.A.; Rötting, T.S.; Macías, F.; Nieto, J.M.; Ayora, C. Field multi-step limestone and MgO passive system to treat acid mine drainage with high metal concentrations. *Appl. Geochem.* **2009**, *24*, 2301–2311. [[CrossRef](#)]
36. Lin, X.; Burns, R.C.; Lawrance, G.A. Heavy metals in wastewater: The effect of electrolyte composition on the precipitation of cadmium (II) using lime and magnesia. *Water Air Soil Poll.* **2005**, *165*, 131–152. [[CrossRef](#)]
37. Sasaki, K.; Fukumoto, N.; Moriyama, S.; Hirajima, T. Sorption characteristics of fluoride on to magnesium oxide-rich phases calcined at different temperatures. *J. Hazard. Mater.* **2011**, *191*, 240–248. [[CrossRef](#)]
38. Moore, R.C.; Anderson, D.R. System for Removal of Arsenic from Water. U.S. Patent 6,821,434B1, 23 November 2004.
39. Navarro, A.; Chimenos, J.; Muntaner, D.; Fernández, I. Permeable reactive barriers for the removal of heavy metals: Lab-scale experiments with low-grade magnesium oxide. *Ground Water Monit. Remediat.* **2006**, *26*, 142–152. [[CrossRef](#)]
40. Rötting, T.S.; Cama, J.; Ayora, C.; Cortina, J.L.; De Pablo, J. Use of caustic magnesia to remove cadmium, nickel, and cobalt from water in passive treatment systems: Column experiments. *Environ. Sci. Technol.* **2006**, *40*, 6438–6443. [[CrossRef](#)] [[PubMed](#)]
41. Ayora, C.; Caraballo, M.A.; Macías, F.; Rötting, T.S.; Carrera, J.; Nieto, J.M. Acid mine drainage in the Iberian Pyrite Belt: 2. Lessons learned from recent passive remediation experiences. *Environ. Sci. Pollut. Res.* **2013**, *20*, 7837–7853. [[CrossRef](#)]
42. Macías, F.; Caraballo, M.A.; Rötting, T.S.; Pérez-López, R.; Nieto, J.M.; Ayora, C. From highly polluted Zn-rich acid mine drainage to non-metallic waters: Implementation of a multi-step alkaline passive treatment system to remediate metal pollution. *Sci. Total Environ.* **2012**, *433*, 323–330. [[CrossRef](#)] [[PubMed](#)]